Qichao Zhang, Zhong-Hai Li, Zhenhan Wu, Xuanhua Chen, Ji'en Zhang, and Yan Yang, 2021, Subduction initiation of the western Proto-Tethys Ocean: New evidence from the Cambrian intra-oceanic forearc ophiolitic mélange in the western Kunlun Orogen, NW Tibetan Plateau: GSA Bulletin, https://doi.org/10.1130/B35922.1.

Supplemental Material

Supplemental File 1. LA-ICPMS zircon U-Pb isotopic analyses for the Qimanyute plagiogranites, FAB-Gs and NEGs in the WKO at the northwestern Tibetan Plateau

Supplemental File 2. SHRIMP zircon U-Pb isotopic analyses for the Qimanyute plagiogranites, FAB-Gs and NEGs in the WKO at the northwestern Tibetan Plateau

Supplemental File 3. Major and trace element data of the Qimanyute plagiogranites, FAB-Gs, boninites and NEGs in the WKO at the northwestern Tibetan Plateau

Supplemental File 4. Sr–Nd isotopic compositions of the Qimanyute plagiogranites, FAB-Gs, boninites and NEGs in the WKO at the northwestern Tibetan Plateau

Supplemental File 5. Pb isotopic compositions of the Qimanyute plagiogranites, FAB-Gs, boninites and NEGs in the WKO at the northwestern Tibetan Plateau

Supplemental File 6. (A) MgO versus Nb/La classification diagram (modified after Kepezhinskas et al., 1996) for the Qimanyute NEGs in the western Kunlun Orogen, NW Tibet. (B) Feldspar normative An–Or–Ab diagram (after O'Connor, 1965) for the Qimanyute plagiogranites, showing the fields for tonalite (To), trondhjemite (Tdh), granodiorite (Gd) and granite (Gr) used in this study. The published data of HNBs and NEBs are from Reagan et al. (1989), Defant et al. (1992), Kepezhinskas et al. (1996), Sajona et al. (1996), Aguillón-Robles et al. (2001), Polat and Kerrich. (2001), Castillo et al. (2002), Gorring et al. (2003), Zhang et al. (2005), Wang et al. (2007, 2008), Petrone and Ferrari, 2008, Macpherson et al. (2010), Hastie et al. (2011), and Sorbadere et al. (2013).

REFERENCES CITED

Andersen, T., 2002, Correction of common lead in U–Pb analyses that do not report ^{204}Pb: Chemical Geology, v. 192, no. 1–2, p. 59–79, https://doi.org/10.1016/S0009-2541(02)00195-X.

Aguillón-Robles, A., Calmus, T., Benoit, M., Bellon, H., Maury, R.C., Cotten, J., Bourgois, J., and Michaud, F., 2001, Late Miocene adakites and Nb-enriched basalts from Vizcaino Peninsula, Mexico: indicators of East Pacific Rise subduction below southern Baja California?: Geology, v. 29, p. 531–534, https://doi.org/10.1130/0091-7613(2001)029<0531:LMAANE>2.0.CO;2.

Castillo, P.R., Solidum, R.U., and Punongbayan, R.S., 2002, Origin of high field strength element enrichment in the Sulu Arc, southern Philippines, revisited: Geology, v. 30, p. 707–710, https://doi.org/10.1130/0091-7613(2002)030<0707:OOHFSE>2.0.CO;2.

Defant, M.J., Jackson, T.E., Drummond, M.S., de Boer, J.Z., Bellon, H., Feigenson, M.D., Maury, R.C., and Stewart, R.H., 1992, The geochemistry of young volcanism throughout western Panama and southeastern Costa Rica: an overview: Journal of the Geological Society, v. 149, p. 569–579, https://doi.org/10.1144/gsjgs.149.4.0569.

Gorring, M., Singer, B., Gowers, J., and Kay, S.M., 2003, Plio–Pleistocene basalts from the Meseta del Lago Buenos Aires, Argentina: evidence for asthenosphere–lithosphere interactions during slab window magmatism: Chemical Geology, v. 193, p. 215–235, https://doi.org/10.1016/S0009-2541(02)00249-8.

Hastie, A.R., Mitchell, S.F., Kerr, A.C., Minifie, M.J., and Millar, I.L., 2011, Geochemistry of rare high-Nb basalt lavas: are they derived from a mantle wedge metasomatised by slab melts?: Geochimica et Cosmochimica Acta, v. 75, p. 5049–5072, https://doi.org/10.1016/j.gca.2011.06.018.

Kepezhinskas, P.K., Defant, M.J., and Drummond, M.S., 1996, Progressive enhancement of island arc mantle by melt–peridotite interaction inferred from Kamchatka adakites: Geochimica et Cosmochimica Acta, v. 60, p. 1217–1229, https://doi.org/10.1016/0016-7037(96)00001-4.

Macpherson, C.G., Chiang, K.K., Hall, R., Nowell, G.M., Castillo, P.R., and Thirlwall, M.F., 2010, Plio-Pleistocene intra-plate magmatism from the southern Sulu Arc, Semporna peninsula, Sabah, Borneo: Implications for high-Nb basalt in subduction zones: Journal of Volcanology and Geothermal Research, v. 190, p. 25–38, https://doi.org/10.1016/j.jvolgeores.2009.11.004.

O’Connor, J.T., 1965, A classification for quartz-rich igneous rock based upon feldspar ratios: U.S. Geological Survey Professional Paper, v. 525B, p. B79–B84.

Petrone, C.M., and Ferrari, L., 2008, Quaternary adakite—Nb-enriched basalt association in the western Trans-Mexican Volcanic Belt: is there any slab melt evidence?: Contributions to Mineralogy and Petrology, v. 156, p. 73–86, https://doi.org/10.1007/s00410-007-0274-9.

Polat, A., and Kerrich, R., 2001, Magnesian andesites, Nb-enriched basaltandesites, and adakites from late-Archean 27 GPa Wana greenstone belts, Superior Province, Canada: implications for late Archean subduction zone petrogenetic processes: Contributions to Mineralogy and Petrology, v. 141, p. 36–52, https://doi.org/10.1007/s004100000223.

Reagan, M.K., and Gill, J.B., 1989, Coexisting calkalkaline and high niobium basalts from Turrialba volcano, Costa Rica: implications for residual titanites in arc magma sources: Journal of Geophysical Research, v. 94, p. 4619–4633, https://doi.org/10.1029/JB094iB04p04619.

Sajona, F.G., Maury, R.C., Bellon, H., Cotten, J., and Defant, M.J., 1996, High field strength element enrichment of Pliocene–Pleistocene island arc basalts, Zamboanga Peninsula, western Mindanao (Philippines): Journal of Petrology, v. 37, p. 693–726, https://doi.org/10.1093/petrology/37.3.693.

Sorbadere, F., Schiano, P., Me’trich, N., and Bertagnini, A., 2013, Small-scale coexistence of island-arc- and enriched-MORB-type basalts in the central Vanuatu arc: Contributions to Mineralogy and Petrology, v. 166, p. 1305–1321, https://doi.org/10.1007/s00410-013-0928-8.

Wang, Q., Wyman, D.A., Zhao, Z.H., Xu, J.F., Bai, Z.H., Xiong, X.L., Dai, T.M., Li, C.F., and Chu, Z.Y., 2007, Petrogenesis of Carboniferous adakites and Nb-enriched arc basalts in the Alataw area, northern Tianshan Range (western China): implications for Phanerozoic crustal growth in the Central Asia orogenic belt: Chemical Geology, v. 236, p. 42–64, https://doi.org/10.1016/j.chemgeo.2006.08.013.

Wang, Q., Wyman, D.A., Xu, J.F., Wan, Y.S., Li, C.F., Zi, F., Jiang, Z.Q., Qiu, H.N., Chu, Z.Y., Zhao, Z.H., and Dong, Y.H., 2008, Triassic Nb-enriched basalts, magnesian andesites, and adakites of the Qiangtang terrane (Central Tibet): evidence for metasomatism by slab-derived melts in the mantle wedge: Contributions to Mineralogy and Petrology, v. 155, p. 473–490, https://doi.org/10.1007/s00410-007-0253-1.

Zhang, H.X., Niu, H.C., Sato, H., Yu, X.Y., Shan, Q., Zhang, B.Y., ITO, J., Nagao, T., 2005, Late Paleozoic adakites and Nb-enriched basalts from northern Xinjiang, northwest China: Evidence for the southward subduction of the Paleo-Asian Oceanic Plate: The Island Arc, v. 14, p. 55–68, https://doi.org/10.1111/j.1440-1738.2004.00457.x.

Supplemental file 1

LA-ICPMSzircon U-Pbisotopic analyses fortheQimanyuteplagiogranites, FAB-Gs and NEGsin the WKOat the northwestern Tibetan Plateau

Spot No.	Elemental data				Corrected Isotopic Ratios						Age (Ma)						
	Pb (ppm)	Th (ppm)	U (ppm)	Th/U	$^{207}Pb^*/^{206}Pb^*$	1σ	$^{207}Pb^*/^{235}U$	1σ	$^{206}Pb^*/^{238}U$	1σ	$^{207}Pb/^{206}Pb$	1σ	$^{207}Pb/^{235}U$	1σ	$^{206}Pb/^{238}U$	1σ	Concordance
QMYT-03(FAB-Gs)																	
1	84	239	1025	0.23	0.0582	0.0010	0.6261	0.0121	0.0780	0.0008	539	35	494	8	484	5	98%
2	57	139	683	0.20	0.0583	0.0015	0.6293	0.0121	0.0784	0.0010	539	57	496	8	487	6	98%
3	72	307	858	0.36	0.0571	0.0007	0.6146	0.0101	0.0780	0.0008	494	23	486	6	484	5	99%
4	101	180	1235	0.15	0.0567	0.0013	0.6199	0.0131	0.0794	0.0006	480	50	490	8	492	4	99%
5	100	581	1135	0.51	0.0578	0.0007	0.6182	0.0086	0.0776	0.0007	524	26	489	5	482	4	98%
6	36	220	424	0.52	0.0561	0.0009	0.6008	0.0130	0.0776	0.0009	454	40	478	8	482	5	99%
7	103	742	1145	0.65	0.0568	0.0005	0.6103	0.0079	0.0779	0.0007	487	20	484	5	484	4	99%
8	113	351	1389	0.25	0.0562	0.0005	0.6039	0.0067	0.0781	0.0007	457	19	480	4	485	4	99%
9	126	225	1558	0.14	0.0549	0.0004	0.5991	0.0070	0.0792	0.0007	409	21	477	4	491	4	97%
10	116	145	1472	0.10	0.0578	0.0007	0.6196	0.0083	0.0779	0.0010	524	26	490	5	484	6	98%
11	89	132	1105	0.12	0.0586	0.0014	0.6268	0.0171	0.0775	0.0009	550	56	494	11	481	6	97%
12	128	701	1554	0.45	0.0559	0.0006	0.5987	0.0107	0.0776	0.0011	450	19	476	7	482	7	98%
13	74	500	845	0.59	0.0555	0.0007	0.5937	0.0085	0.0777	0.0008	432	-5	473	5	482	5	98%
14	134	473	1614	0.29	0.0554	0.0007	0.5977	0.0106	0.0782	0.0012	428	-5	476	7	486	7	97%
15	96	369	1148	0.32	0.0581	0.0009	0.6207	0.0115	0.0772	0.0010	600	35	490	7	479	6	97%
16	858	984	5365	0.18	0.0575	0.0004	0.6188	0.0075	0.0781	0.0008	509	18	489	5	485	5	99%
17	331	480	766	0.63	0.0564	0.0004	0.6153	0.0061	0.0791	0.0006	478	18	487	4	491	4	99%
18	738	1015	2576	0.39	0.0567	0.0003	0.6137	0.0058	0.0785	0.0006	480	14	486	4	487	4	99%
19	367	530	1074	0.49	0.0562	0.0003	0.6119	0.0057	0.0789	0.0006	461	25	485	4	490	4	99%
20	142	206	371	0.56	0.0563	0.0004	0.6139	0.0064	0.0791	0.0006	465	25	486	4	491	4	99%
21	244	331	871	0.38	0.0560	0.0004	0.6155	0.0065	0.0796	0.0006	454	7	487	4	494	4	98%

Note: *=radiogenic Pb. Isotopic ratios are presented with 1σ uncertainties. Common lead corrected using the method of Anderson (2002). FAB-G: forearc basalt-like gabbro; NEG: Nb-enriched gabbro.

Supplemental file 2

SHRIMP zircon U-Pb isotopic analyses for theQimanyuteplagiogranites, FAB-Gs and NEGs in the WKO at the northwestern Tibetan Plateau

Spot No.					Corrected Isotopic Ratios						Age (Ma)					
	Th (ppm)	U (ppm)	Th/U	$^{206}Pb^*$ (ppm)	$^{207}Pb^*/^{206}Pb^*$	±%	$^{207}Pb^*/^{235}U$	±%	$^{206}Pb^*/^{238}U$	±%	$^{207}Pb^*/^{206}Pb^*$	1σ	$^{208}Pb^*/^{232}Th$	1σ	$^{206}Pb^*/^{238}U$	1σ
QMYTHC-03(plagiogranites)																
1	2948	744	0.26	204	0.0571	0.7	0.6340	1.5	0.0805	1.3	495	15	485	8	499	7
2	1467	394	0.28	101	0.0541	5.1	0.5820	5.3	0.0780	1.4	374	110	438	41	484	7
3	2439	913	0.39	167	0.0573	0.8	0.6289	1.6	0.0797	1.4	501	18	486	8	494	6
4	584	108	0.19	41	0.0577	1.5	0.6450	2.0	0.0811	1.4	519	32	514	13	503	7
5	1005	255	0.26	69	0.0566	2.7	0.6150	3.0	0.0787	1.4	478	59	478	24	489	7
6	1018	219	0.22	69	0.0573	1.2	0.6240	1.8	0.0791	1.4	501	25	490	10	491	7
7	2008	662	0.34	139	0.0564	1.0	0.6250	1.7	0.0804	1.4	468	23	479	9	499	7
8	2366	460	0.20	162	0.0570	1.6	0.6220	2.1	0.0791	1.4	491	35	580	22	491	6
QMYTX-05(NEGs)																
1	835	406	0.50	56	0.0551	1.5	0.5950	2.1	0.0782	1.4	417	34	480	9	486	7
2	502	481	0.99	34	0.0554	2.1	0.5940	2.6	0.0777	1.4	430	47	470	9	482	7
3	556	485	0.90	37	0.0553	1.9	0.5910	2.4	0.0776	1.4	423	42	473	9	482	7
4	700	440	0.65	48	0.0556	1.7	0.6060	2.2	0.0790	1.4	437	38	481	11	490	7
5	653	805	1.27	43	0.0565	1.6	0.5940	2.2	0.0762	1.4	473	36	466	8	474	7
6	403	421	1.08	27	0.0555	2.7	0.6000	3.0	0.0784	1.5	432	59	486	10	486	7
7	709	840	1.22	48	0.0550	3.2	0.5910	3.5	0.0778	1.4	414	72	467	8	483	7
8	650	254	0.40	44	0.0576	1.5	0.6190	2.1	0.0780	1.4	513	33	527	11	484	7
9	501	442	0.91	34	0.0552	2.2	0.5980	2.6	0.0786	1.4	420	48	481	9	488	7
10	494	460	0.96	33	0.0565	1.8	0.6070	2.3	0.0780	1.4	472	40	484	9	484	7
11	926	84	0.09	63	0.0545	1.9	0.5950	2.3	0.0792	1.4	392	42	397	34	491	7
12	632	56	0.09	43	0.0578	1.8	0.6320	2.3	0.0792	1.4	523	39	504	29	492	7

Note: *=radiogenic Pb.$^{206}Pb_c$ indicates the common lead portion. Common Pb corrected using measured ^{204}Pb. Errors are 1-sigma.

Supplemental file 3

Major and trace element data of theQimanyuteplagiogranites, FAB-Gs, boninites and NEGs in the WKO at the northwestern Tibetan Plateau

Pluton	QMYT(FAB-G)																	
Sample	QMYT-01	QMYT-02	QMYT-03	QMYT-04	QMYT-05	QMYT-07	QMYT-09	QMYT-10	QMYT-11	QMYT-12	QMYT-13	QMYT-14	QMYT-15	QMYT-16	QMYT-17	QMYT-18	QMYT-21	QMYT-2
lajor elements (wt.%)																		
SiO_2	46.67	50.14	51.30	48.46	51.27	51.43	47.94	46.90	47.95	48.35	48.24	50.71	47.85	48.39	51.57	51.38	50.42	52.73
TiO_2	0.88	1.19	0.97	2.03	0.57	0.48	0.89	0.89	1.24	1.28	1.00	1.01	2.15	2.12	0.57	0.57	0.50	0.47
Al_2O_3	15.71	13.98	13.96	14.19	13.99	14.66	15.46	15.95	14.39	14.28	14.19	14.28	14.32	14.40	14.07	14.08	14.99	14.55
$^{T}Fe_2O_3$	10.69	11.43	11.56	12.97	8.73	8.70	10.44	10.39	11.62	11.50	11.60	11.68	13.06	12.49	8.72	8.79	8.74	7.96
MnO	0.16	0.18	0.18	0.20	0.14	0.15	0.16	0.15	0.18	0.18	0.17	0.18	0.19	0.18	0.14	0.14	0.15	0.14
MgO	8.60	6.08	6.10	6.06	7.90	8.74	7.94	8.04	6.00	5.84	5.91	5.99	5.88	5.81	7.56	7.57	8.25	7.68
CaO	12.50	10.39	8.67	10.42	12.68	10.47	12.58	13.19	11.04	10.95	9.07	9.09	10.77	10.92	13.11	13.11	10.98	10.66
Na_2O	1.89	3.53	4.00	3.21	2.61	3.27	1.90	1.95	3.68	3.64	4.08	4.03	3.14	3.14	2.74	2.73	3.45	3.29
K_2O	0.07	0.24	0.42	0.23	0.11	0.27	0.05	0.04	0.24	0.25	0.42	0.42	0.21	0.20	0.09	0.09	0.29	0.26
P_2O_5	0.01	0.04	0.02	0.03	0.01	0.01	0.15	0.16	0.09	0.09	0.13	0.10	0.14	0.13	0.24	0.25	0.12	0.11
LOI	2.51	2.33	2.36	2.01	1.54	2.17	1.68	1.63	2.32	2.35	4.36	1.58	1.13	1.22	0.37	0.32	1.36	1.22
Total	99.69	99.53	99.54	99.81	99.55	100.35	99.17	99.30	98.74	98.69	99.17	99.07	98.84	99.01	99.19	99.04	99.23	99.06
Mg#	0.62	0.52	0.51	0.48	0.64	0.67	0.60	0.61	0.51	0.50	0.50	0.51	0.47	0.48	0.63	0.63	0.65	0.66
arce elements (ppm)																		
Li	8.79	7.44	9.95	8.12	2.68	8.2	8.64	8.54	7.51	7.45	9.88	9.87	8.25	8.09	2.79	2.77	8.36	8.23
P	63.3	218	117	146	47.5	43.4	67.3	67.6	235	238	137	137	168	161	73.5	69.8	70.6	67.8
Ca	91400	75200	62400	75800	91300	74800	92600	92300	76400	76900	63500	63400	76600	76100	94700	94300	76400	76300
Sc	44.9	36	35.8	47.4	38.3	40.9	44.7	44.4	36.1	36.2	36	35.9	47.4	46.8	39.2	39	41.6	41.4
Ti	5070	7110	5600	12300	3130	2630	5210	5190	7150	7190	5790	5780	13100	13000	3350	3340	2770	2770
V	327	263	246	320	253	231	321	321	258	261	242	241	297	293	254	254	229	229
Cr	381	234	205	187	325	663	370	371	227	228	200	200	183	181	326	324	655	654
Mn	1280	1450	1440	1550	1100	1170	1290	1290	1460	1470	1450	1440	1560	1550	1120	1120	1170	1170
Co	49.2	35.5	34.6	36.5	39.6	44.4	49.1	49.2	35.4	35.5	34.6	34.5	36.3	36	40.3	40.3	45.1	44.9
Ni	126	64.8	59.2	52.8	95.9	118	124	125	64.4	64.7	59.5	58.8	52.2	51.9	97.3	96.8	118	118

Cu	45.6	10.9	18.2	26.8	117	34	46.7	46.7	14.2	14.2	20.5	20.4	31.8	31.7	117	117	34.6	34.5
Zn	59.5	72	75.4	73.4	43.1	52.6	60	60.1	72.5	72.5	74.8	74.8	76.5	76.4	43.9	43.6	51.6	51.3
Ga	16.7	16.5	15.5	19	15.1	14.1	16.9	16.7	16.6	16.5	15.5	15.4	18.8	18.7	15.4	15.3	14.1	14.1
Rb	1.16	6.32	13.2	6.47	2.34	7.02	0.901	0.91	6.29	6.24	13.1	13.1	6.43	6.39	2.36	2.32	7.06	7.04
Sr	196	147	121	159	216	192	194	193	150	146	121	121	158	157	221	219	192	191
Y	12.6	27.1	25.7	24.4	9.73	7.28	12.6	12.5	27	27	25.8	25.6	24.3	24.2	9.86	9.86	7.27	7.25
Zr	7.56	22.3	12.7	14.2	4.98	5.8	7.86	7.87	25.3	24	17.1	16.8	16.3	15	5.41	5.41	6.11	6.11
Nb	0.0916	1.05	0.922	0.879	0.0374	0.0886	0.0734	0.0728	1.07	1.07	0.941	0.931	0.892	0.9	0.048	0.0465	0.0998	0.094
Sn	0.263	0.303	0.263	0.341	0.344	0.392	0.168	0.169	0.215	0.219	0.197	0.204	0.259	0.263	0.256	0.252	0.352	0.358
Cs	0.103	0.438	1.07	0.663	0.0974	0.335	0.103	0.105	0.45	0.45	1.08	1.08	0.676	0.666	0.102	0.101	0.344	0.342
Ba	7.91	97.8	163	77	15.3	66.8	8.02	7.88	99.3	97.7	164	164	76.7	76.9	15.6	15.6	67.5	67.3
La	0.458	2.31	1.88	1.89	0.383	0.482	0.455	0.456	2.27	2.27	1.98	1.95	1.87	1.89	0.41	0.395	0.492	0.486
Ce	1.4	7.08	5.98	5.8	1.06	1.2	1.41	1.4	6.99	7.02	6.12	6.11	5.75	5.82	1.11	1.09	1.2	1.21
Pr	0.315	1.23	1.07	1.02	0.227	0.225	0.309	0.309	1.21	1.21	1.09	1.08	0.996	1.01	0.237	0.235	0.235	0.23
Nd	2.17	6.9	6.01	5.74	1.58	1.41	2.15	2.18	6.78	6.74	6.08	6.09	5.73	5.74	1.63	1.61	1.42	1.44
Sm	1.03	2.49	2.24	2.23	0.771	0.626	1.07	1.07	2.56	2.55	2.29	2.28	2.25	2.25	0.803	0.805	0.647	0.624
Eu	0.71	1.03	0.857	1.1	0.544	0.43	0.712	0.705	1.02	1.02	0.857	0.854	1.09	1.08	0.553	0.544	0.437	0.43
Gd	1.73	3.65	3.26	3.37	1.32	1	1.71	1.72	3.6	3.58	3.24	3.23	3.33	3.33	1.31	1.31	1.01	1
Tb	0.33	0.678	0.616	0.628	0.251	0.192	0.331	0.328	0.679	0.675	0.626	0.627	0.626	0.633	0.26	0.261	0.196	0.194
Dy	2.19	4.46	4.08	4.14	1.7	1.27	2.17	2.18	4.41	4.43	4.07	4.08	4.07	4.06	1.69	1.7	1.26	1.27
Ho	0.471	0.966	0.904	0.887	0.368	0.274	0.472	0.469	0.965	0.97	0.906	0.9	0.884	0.884	0.372	0.372	0.273	0.271
Er	1.32	2.78	2.62	2.49	1.01	0.75	1.32	1.32	2.79	2.79	2.65	2.64	2.51	2.5	1.03	1.03	0.763	0.757
Tm	0.196	0.427	0.41	0.381	0.15	0.111	0.194	0.195	0.427	0.429	0.416	0.416	0.384	0.382	0.152	0.153	0.113	0.113
Yb	1.21	2.67	2.6	2.41	0.898	0.678	1.22	1.21	2.72	2.71	2.69	2.67	2.44	2.44	0.935	0.931	0.685	0.684
Lu	0.181	0.413	0.413	0.382	0.136	0.101	0.181	0.183	0.415	0.414	0.418	0.413	0.381	0.381	0.141	0.139	0.104	0.104
Hf	0.388	0.948	0.701	0.696	0.257	0.265	0.404	0.393	1.01	0.984	0.83	0.824	0.749	0.708	0.267	0.271	0.27	0.274
Ta	0.0176	0.0568	0.0538	0.0494	0.0038	0.0073	0.0091	0.0091	0.0583	0.0589	0.0563	0.056	0.0519	0.0512	0.0111	0.0099	0.0187	0.0183
Pb	4.18	2.35	1.51	2.83	5.18	4.83	3.54	3.52	1.72	1.65	1.24	1.25	2.18	2.19	4.44	4.43	4.11	4.06
Th	0.0689	0.0689	0.0907	0.0902	0.0495	0.0661	0.0596	0.0594	0.0637	0.0672	0.0949	0.097	0.0879	0.0889	0.0466	0.0476	0.063	0.0658
U	0.104	0.163	0.201	0.33	0.162	0.24	0.102	0.101	0.159	0.166	0.214	0.209	0.336	0.333	0.163	0.165	0.245	0.242
La/Yb)$_N$	0.27	0.62	0.52	0.56	0.31	0.51	0.27	0.27	0.60	0.60	0.53	0.52	0.55	0.56	0.31	0.30	0.52	0.51

δEu	1.62	1.04	0.97	1.22	1.64	1.66	1.60	1.58	1.03	1.03	0.96	0.96	1.22	1.20	1.64	1.61	1.65	1.66

Note:Mg# = [atomic MgO/(MgO+FeO)]. FAB-G:forearc basalt-like gabbro; NEG:Nb-enriched gabbro.

Continued Supplemental file 3

QMYTH(boninite)											QMYTX(NEG)			
QMYTH-01	QMYTH-02	QMYTH-03	QMYTH-04	QMYTH-05	QMYTH-06	QMYTH-07	QMYTH-08	QMYTH-09	QMYTH-10	QMYTH-11	QMYTX-01	QMYTX-02	QMYTX-03	QMYTX-04
Major elements (wt.%)														
54.57	52.99	62.42	58.21	52.16	51.64	55.89	53.4	56.01	54.92	55.18	46.88	46.18	52.8	56.32
0.25	0.14	0.43	0.31	0.58	0.24	0.53	0.13	0.37	0.18	0.18	0.78	1.17	0.57	0.74
13.43	9.92	12.56	13.87	14.50	14.78	15.21	9.8	15.19	11.36	11.54	16.03	15.75	15.79	17.85
10.34	8.78	8.73	10.74	10.25	9.88	10.19	11.06	10.31	10.26	10.35	11.87	12.85	8.99	6.17
0.18	0.09	0.13	0.16	0.17	0.16	0.16	0.2	0.15	0.15	0.15	0.21	0.17	0.21	0.09
8.07	12.91	4.65	4.91	7.29	8.70	5.91	11.21	5.51	10.51	10.02	8.17	5.85	7.15	4.07
9.43	10.62	6.88	7.90	10.24	10.24	8.19	11.44	7.87	9.07	8.98	11.41	12.07	8.73	6.55
2.44	2.35	2.87	2.73	3.35	2.90	2.77	1.26	2.8	1.86	1.86	2.06	2.14	3.12	3.83
0.14	0.09	0.08	0.13	0.15	0.22	0.13	0.17	0.13	0.15	0.16	0.88	0.96	0.65	2.79
0.03	0.01	0.03	0.04	0.04	0.01	0.04	0.02	0.03	0.01	0.01	0.08	0.22	0.09	0.2
0.61	1.46	1.03	0.40	0.66	0.79	0.72	1.18	1.02	0.99	0.93	1.09	1.88	1.02	0.9
99.49	99.36	99.81	99.40	99.39	99.56	99.74	99.87	99.39	99.46	99.36	99.46	99.24	99.12	99.51
0.61	0.75	0.52	0.48	0.59	0.64	0.54	0.67	0.52	0.67	0.66	0.58	0.48	0.61	0.57
Tarce elements (ppm)														
2.86	4.03	3.2	2.69	1.81	3.32	3.55	1.89	4.62	3.11	3.07	27.8	24.2	24.6	23.9
223	124	195	255	259	153	238	177	206	162	170	478	1060	459	876
69900	77400	49100	56700	75200	73100	59400	83500	56900	66600	66200	83500	86900	64200	46300
46.9	44.4	30.9	42.1	43.4	44.5	39.6	44.2	42.9	43.9	44.3	43.4	43.3	35.5	18.7
1400	773	2370	1730	3340	1300	3060	756	2110	989	992	4610	6960	3250	4030
258	214	234	255	285	304	262	229	280	235	239	314	345	198	123
435	1180	84.4	139	184	358	178	1970	40.2	653	579	60	10.6	179	68.3
1370	728	1010	1260	1330	1230	1210	1630	1140	1180	1200	1610	1330	1590	636

43.3	28.6	28.3	34.3	39.2	41.5	33.9	54.2	34.1	46.2	45.5	48.8	44.3	33.8	20.6
109	210	31.1	28.1	59.6	91.8	48.1	158	27.2	96.7	91.2	61.2	29.3	81.7	28.1
19.3	0.363	47	49.5	16.6	13.6	40.5	17.7	14.4	59.8	56.9	20.1	185	55.6	44
95.7	17.5	58.2	69.7	82.9	59.3	72.7	98.8	55	69.8	70.2	133	124	202	78
11.9	9.23	11.6	13.1	10.9	13.2	14.3	8.73	12.8	9.94	10.1	17.2	19	14.6	20.1
1.85	1.09	0.59	0.605	0.575	2.02	1.21	2.14	1.5	1.52	1.49	29.8	33.4	26.7	76.6
85.2	75.3	98.4	112	93.5	108	112	55.1	87.6	57.3	57.4	349	526	365	536
8.41	7.56	12.5	9.83	15.2	7.63	13.5	5.27	10.2	6.09	6.66	22.2	34.7	16.2	40.8
17.4	7.24	21.2	26.5	28.8	8.55	25.9	7.38	13.7	7.8	7.87	58.7	89.2	56.9	235
0.64	0.211	0.386	0.92	0.567	0.108	0.502	0.0882	0.203	0.096	0.0972	2.49	4.91	3.3	8.75
0.347	1.07	0.419	0.314	0.438	0.241	0.412	0.215	0.307	0.189	0.195	1.34	2.14	1.59	2.12
0.132	0.0967	0.104	0.0995	0.0925	0.237	0.15	0.259	0.283	0.223	0.201	1.32	3.07	3.14	2.91
29	13	26.3	32.6	33.5	29.5	18.5	21.4	36.5	19.2	19.8	249	649	250	792
1.49	0.828	1.25	2.13	1.37	0.433	1.26	0.437	0.874	0.404	0.453	16.6	59.3	15.1	53.2
3.4	2.78	3.17	4.87	3.71	1.21	3.59	1.07	2.14	1.02	1.12	33.6	112	30.1	102
0.476	0.456	0.512	0.673	0.61	0.196	0.549	0.153	0.342	0.157	0.167	4.06	12.4	3.64	11.4
2.25	2.25	2.7	3.12	3.26	1.1	3.01	0.789	1.85	0.852	0.924	16.1	45.6	14.2	41.2
0.709	0.679	1.01	0.944	1.24	0.456	1.11	0.301	0.715	0.35	0.373	3.48	8.17	2.91	7.58
0.25	0.22	0.396	0.315	0.409	0.186	0.433	0.133	0.298	0.137	0.141	1.01	1.96	0.809	1.46
0.98	0.918	1.51	1.23	1.84	0.77	1.67	0.499	1.14	0.589	0.645	3.57	6.91	2.78	6.91
0.186	0.171	0.29	0.225	0.352	0.158	0.315	0.102	0.225	0.119	0.131	0.591	1.05	0.452	1.08
1.27	1.19	1.96	1.49	2.39	1.13	2.14	0.745	1.58	0.873	0.951	3.67	6	2.74	6.44
0.298	0.287	0.452	0.345	0.548	0.278	0.491	0.182	0.372	0.216	0.237	0.797	1.22	0.567	1.35
0.919	0.899	1.34	1.08	1.65	0.859	1.46	0.588	1.13	0.688	0.741	2.29	3.34	1.59	3.99
0.151	0.154	0.214	0.179	0.264	0.141	0.235	0.0992	0.185	0.115	0.121	0.349	0.505	0.241	0.638
1.04	1.04	1.4	1.2	1.7	0.944	1.54	0.702	1.24	0.791	0.813	2.23	3.17	1.5	4.09
0.17	0.163	0.218	0.199	0.272	0.155	0.243	0.118	0.196	0.13	0.133	0.341	0.481	0.226	0.628
0.532	0.232	0.694	0.762	0.931	0.321	0.848	0.243	0.484	0.27	0.278	1.61	2.34	1.49	5.68
0.0342	0.0104	0.0278	0.0445	0.0383	0.00842	0.0347	0.00682	0.0136	0.00733	0.00762	0.104	0.251	0.182	0.737
1.42	0.367	1.67	0.752	1.51	0.579	0.843	0.452	1.14	0.654	0.622	9.26	17.4	15.8	19.9
0.222	0.0971	0.144	0.342	0.181	0.0572	0.157	0.0459	0.0986	0.0508	0.0563	3.51	14.4	3.72	26.2

0.183	0.218	0.0983	0.258	0.17	0.148	0.107	0.0864	0.161	0.0958	0.104	0.461	1.31	0.871	10.5
1.03	0.57	0.64	1.27	0.58	0.33	0.59	0.45	0.51	0.37	0.40	5.34	13.42	7.22	9.33
0.92	0.85	0.98	0.89	0.83	0.95	0.97	1.04	1.01	0.92	0.87	0.87	0.78	0.86	0.61

Continued Supplemental file 3

QMYTX(NEG)						QMYTHC(plagiogranite)				
QMYTX-05	QMYTX-06	QMYTX-07	QMYTX-08	QMYTX-09	QMYTX-10	QMYTHC-01	QMYTHC-02	QMYTHC-03	QMYTHC-04	QMYTHC-05
Major elements (wt.%)										
51.38	50.02	48.92	52.44	51.28	49.21	73.3	72.45	73.28	72.18	73.38
1.09	1	1.13	0.94	0.87	1.01	0.3	0.29	0.28	0.28	0.29
15.98	16.79	16.07	16.51	16.88	16.18	11.15	11.09	11.02	10.71	10.9
11.72	11.84	11.90	11.18	10.73	11.70	7.02	6.41	6.75	7.42	6.71
0.19	0.22	0.2	0.22	0.21	0.21	0.09	0.08	0.08	0.09	0.09
5.49	6.14	6.39	5.6	5.94	6.54	0.3	0.25	0.27	0.3	0.27
6.79	7.18	7.62	6.35	6.95	8.02	3.24	5.04	3.42	2.88	2.75
3.29	3.43	2.91	3.54	3.69	2.84	3.98	3.44	3.93	3.92	4.01
1.31	1.19	1.5	1.29	1.13	1.14	0.16	0.13	0.16	0.32	0.24
0.29	0.13	0.31	0.09	0.12	0.28	0.07	0.07	0.07	0.07	0.07
1.4	1.25	1.7	1.33	1.25	1.79	1.19	1.25	1.05	2.38	2.01
98.93	99.19	98.65	99.49	99.05	98.92	100.80	100.50	100.31	100.55	100.72
0.48	0.51	0.52	0.50	0.53	0.53	0.08	0.07	0.07	0.07	0.07
Tarce elements (ppm)										
46.1	40.7	42.1	41	41.4	44.2	2.6	2.33	2.3	4.38	3.89
1280	620	1490	441	599	1390	348	352	345	317	329
48900	52300	55600	44900	50100	58200	21300	34500	22500	18800	17800
32.6	40.8	35	37.2	37.8	36.1	27.3	25.9	26	26.3	27
6480	5930	6740	5400	5080	6040	1620	1620	1560	1530	1590
263	289	281	262	259	274	0.718	0.608	0.549	0.695	0.532
56.3	32.1	46.7	25.7	56.4	74.1	0.568	0.311	0.24	0.284	0.166

1420	1690	1560	1630	1600	1610	624	585	600	669	619
44	43.8	34.9	43.9	48.2	39.1	2.98	2.63	2.62	2.61	2.41
34.3	37.9	42.3	34.4	45.5	50.5	0.255	0.306	0.205	0.236	0.17
137	126	190	179	111	147	1.98	0.461	0.743	0.888	1.13
196	221	217	208	218	244	29.7	22.4	26.6	42.8	39.7
19.1	19	19.5	18.6	18.5	18.8	10.1	11.6	10	10	9.7
72.7	61.4	92.5	67.4	58.9	62.7	2.98	1.73	2.58	5.88	4.33
414	315	484	284	280	446	101	137	105	78.6	71.8
31.9	27.6	26.3	26.8	25.5	24.4	22.9	18.5	20.6	19.8	19.7
185	72.5	179	75.6	86.8	159	3.23	3.54	2.96	3.41	3.43
6.25	4.61	6.63	5.56	4.84	5.44	1.51	1.28	1.36	1.35	1.38
2.89	3.08	2.95	3.04	2.48	2.83	1.27	1.3	1.22	1.57	1.52
8.62	7.96	9.81	7.65	6.92	7.04	0.577	0.625	0.59	0.42	0.326
511	389	834	421	415	598	63.6	38.6	64.2	103	71.8
81	14.6	59.2	15.7	17.9	54.5	3.86	4.31	4.48	4.46	3.07
153	32	117	34.7	37.6	107	9.19	9.37	9.85	9.17	7.43
15.9	4.05	12.8	4.4	4.52	11.6	1.31	1.24	1.33	1.21	1.08
54.9	16.9	47.5	18.2	18.2	42.7	6.28	5.78	6.17	5.61	5.29
8.27	3.93	7.81	4.15	4.02	7.02	1.97	1.64	1.8	1.72	1.67
1.76	1.16	1.75	1.13	1.09	1.69	0.488	0.531	0.5	0.555	0.698
6.36	4.21	6.04	4.31	4.09	5.52	2.71	2.2	2.43	2.35	2.27
0.949	0.726	0.862	0.733	0.688	0.794	0.511	0.411	0.457	0.446	0.431
5.43	4.52	4.7	4.47	4.24	4.34	3.5	2.81	3.15	3.06	2.94
1.11	0.958	0.911	0.935	0.885	0.851	0.816	0.66	0.73	0.711	0.693
3.11	2.79	2.49	2.69	2.55	2.3	2.52	2.07	2.28	2.21	2.16
0.466	0.433	0.367	0.413	0.392	0.339	0.42	0.347	0.38	0.366	0.358
2.94	2.76	2.29	2.6	2.48	2.09	2.74	2.34	2.54	2.45	2.39
0.438	0.417	0.334	0.395	0.378	0.311	0.428	0.376	0.403	0.389	0.375
4.27	2.06	3.99	2.24	2.4	3.58	0.175	0.191	0.166	0.19	0.191
0.374	0.301	0.294	0.388	0.363	0.221	0.0707	0.0626	0.0673	0.0611	0.0628
25.6	16.2	29.3	17.9	17.2	24.2	0.681	1.01	0.641	1.18	0.747

18.1	3.24	12.6	6.41	7.28	12.4	0.313	0.371	0.364	0.457	0.341
2.15	1.32	2.67	2.31	1.97	2.08	0.154	0.182	0.163	0.158	0.146
19.76	3.79	18.54	4.33	5.18	18.70	1.01	1.32	1.27	1.31	0.92
0.71	0.87	0.75	0.81	0.81	0.80	0.65	0.85	0.73	0.84	1.10

Supplemental file 4

Sr–Ndisotopic compositions of the Qimanyute plagiogranites, FAB-Gs, boninites and NEGs in the WKO at the northwestern Tibetan Plateau

Sample	Pluton	Rb (ppm)	Sr (ppm)	$^{87}Rb/^{86}Sr$	$^{87}Sr/^{86}Sr$	2σm	Sr_i	Sm (ppm)	Nd (ppm)	$^{147}Sm/^{144}Nd$	$^{143}Nd/^{144}Nd$	2σm	$f_{Sm/Nd}$	$\varepsilon_{Nd}(t)$
QMYT-01	FAB-G	1.16	196	0.02	0.711009	9	0.7109	1.03	2.17	0.2889	0.513320	6	0.35	7.6
QMYT-02		6.32	147	0.12	0.705210	10	0.7044	2.49	6.90	0.2196	0.513065	5	0.03	6.9
QMYT-03		13.20	121	0.32	0.705653	12	0.7035	2.24	6.01	0.2268	0.513077	5	0.06	6.7
QMYT-04		6.47	159	0.12	0.705697	9	0.7049	2.23	5.74	0.2365	0.513117	5	0.11	6.9
QMYT-05		2.28	216	0.03	0.710274	8	0.7101	0.77	1.58	0.2970	0.513305	9	0.39	6.8
QMYT-07		7.02	192	0.11	0.711580	7	0.7109	0.63	1.41	0.2702	0.513219	7	0.27	6.8
QMYT-09		0.90	194	0.01	0.710996	9	0.7109	1.07	2.15	0.3029	0.513344	8	0.42	7.2
QMYT-11		6.29	150	0.12	0.705234	9	0.7044	2.56	6.78	0.2298	0.513087	5	0.08	6.7
QMYT-13		13.10	121	0.31	0.705626	9	0.7035	2.29	6.08	0.2292	0.513073	5	0.07	6.5
QMYT-21		4.98	74	0.20	0.708675	9	0.7073	0.65	2.25	0.1750	0.512864	6	-0.18	5.8
QMYT-22		4.96	74	0.19	0.708676	9	0.7073	0.65	2.23	0.1774	0.512871	7	-0.17	5.8
QMYTH-01	boninite	1.85	85	0.06	0.705810	7	0.7054	0.71	2.25	0.1918	0.512969	13	-0.10	6.8
QMYTH-02		1.09	75	0.04	0.706260	7	0.7060	0.68	2.25	0.1837	0.512983	14	-0.14	7.5
QMYTH-03		0.59	98	0.02	0.705972	7	0.7059	1.01	2.70	0.2277	0.513136	11	0.07	7.8
QMYTH-04		0.61	112	0.02	0.705511	7	0.7054	0.94	3.12	0.1841	0.512923	11	-0.14	6.3
QMYTH-05		0.58	94	0.02	0.706083	8	0.7060	1.24	3.26	0.2315	0.513104	10	0.08	6.9
QMYTX-01	NEG	29.80	349	0.25	0.711250	8	0.7095	3.48	16.10	0.1316	0.512330	7	-0.38	-2.0
QMYTX-02		33.40	526	0.18	0.712887	7	0.7116	8.17	45.60	0.1090	0.512227	10	-0.49	-2.6
QMYTX-03		26.70	365	0.21	0.713661	8	0.7122	2.91	14.20	0.1247	0.512299	14	-0.42	-2.2
QMYTX-05		72.70	414	0.51	0.715798	7	0.7123	8.27	54.90	0.0917	0.512046	9	-0.57	-5.0
QMYTHC-01	plagiogranite	2.98	101	0.09	0.705893	6	0.7053	1.97	6.28	0.1909	0.512890	7	-0.11	5.3
QMYTHC-02		1.73	137	0.04	0.705702	6	0.7054	1.64	5.78	0.1727	0.512858	11	-0.19	5.8
QMYTHC-03		2.58	105	0.07	0.705830	8	0.7053	1.80	6.17	0.1776	0.512886	10	-0.17	6.0

Note: $\varepsilon_{Nd}=((^{143}Nd/^{144}Nd)_s/(^{143}Nd/^{144}Nd)_{CHUR}-1)\times10000$, $f_{Sm/Nd}=(^{147}Sm/^{144}Nd)_s/(^{147}Sm/^{144}Nd)_{CHUR}-1$, wheres =sample, $(^{143}Nd/^{144}Nd)_{CHUR}=0.512638$, and $(^{147}Sm/^{144}Nd)_{CHUR}=0.1967$.

Supplemental file 5

Pb isotopic compositions of the Qimanyuteplagiogranites, FAB-Gs, boninites and NEGs in the WKO at the northwestern Tibetan Plateau

Sample	Pluton	Pb/ppm	Th/ppm	U/ppm	$^{208}Pb/^{204}Pb$	$^{207}Pb/^{204}Pb$	$^{206}Pb/^{204}Pb$	$(^{208}Pb/^{204}Pb)_t$	$(^{207}Pb/^{204}Pb)_t$	$(^{206}Pb/^{204}Pb)_t$
QMYT-1	FAB-G	4.18	0.0689	0.1040	38.4491	15.6571	18.6924	38.4194	15.6489	18.5494
QMYT-2		2.35	0.0689	0.1630	38.3084	15.6320	18.4879	38.2559	15.6094	18.0912
QMYT-3		1.51	0.0907	0.2010	38.4225	15.6443	18.6188	38.3146	15.6009	17.8547
QMYT-4		2.83	0.0902	0.3300	38.3466	15.6390	18.5566	38.2894	15.601	17.8885
QMYT-5		5.26	0.0487	0.1650	38.4702	15.6587	18.6568	38.4536	15.6484	18.4764
QMYT-7		4.83	0.0637	0.2460	38.5250	15.6636	18.7594	38.5012	15.6469	18.466
QMYT-09		3.54	0.0596	0.1020	38.4680	15.6619	18.6845	38.4377	15.6525	18.5188
QMYT-11		1.72	0.0637	0.1590	38.3902	15.6479	18.5931	38.3237	15.6177	18.0628
QMYT-13		1.24	0.0949	0.2140	38.4647	15.6530	18.6712	38.327	15.5965	17.6792
QMYTH-01	boninite	1.42	0.2220	0.1830	38.4792	15.6838	19.3876	38.1962	15.6414	18.6424
QMYTH-02		0.37	0.0971	0.2180	38.5016	15.7888	20.9739	38.0116	15.5889	17.4599
QMYTH-03		1.67	0.1440	0.0983	38.4645	15.6580	18.9689	38.3094	15.6387	18.6306
QMYTH-04		0.75	0.3420	0.2580	38.5848	15.7016	19.9807	37.7535	15.5877	17.9776
QMYTH-05		1.51	0.1810	0.1700	38.4006	15.6683	19.1961	38.1844	15.6314	18.5475
QMYTX-01	NEG	9.26	3.5100	0.4610	39.3094	15.6725	18.6251	38.6226	15.6561	18.337
QMYTX-02		17.40	14.4000	1.3100	40.2802	15.6913	18.9463	38.7544	15.6661	18.5029
QMYTX-03		15.80	3.7200	0.8710	38.8507	15.6835	18.8714	38.4252	15.6654	18.5532
QMYTX-05		25.60	18.1000	2.1500	39.4776	15.6953	19.0761	38.1856	15.6674	18.5858
QMYTHC-01	plagiogranite	0.68	0.3130	0.1540	39.1446	15.8193	21.4083	38.2648	15.7403	20.0249
QMYTHC-02		1.01	0.3710	0.1820	38.7339	15.7022	19.4352	38.0535	15.6413	18.3684
QMYTHC-03		0.64	0.3640	0.1630	39.0581	15.7122	19.6150	37.9989	15.6257	18.0993

Note:InitialPbisotope ratios were calculated by LA-ICP-MS and SHRIMP zircon U-Pb data. $(^{208}Pb/^{204}Pb)_i=(^{208}Pb/^{204}Pb)_{measured}-\mu/(e^{\lambda t}-1)$, $(^{207}Pb/^{204}Pb)_i=(^{207}Pb/^{204}Pb)_{measured}-\mu/137.88(e^{\lambda t}-1)$, $(^{206}Pb/^{204}Pb)_i=(206Pb/204Pb)_{measured}-\omega(e^{\lambda t}-1)$, $\lambda^{238}U=1.55125*10^{-10}/a$, $\lambda^{235}U=9.8485*10^{-10}/a$, $\lambda^{232}Th=4.9475*10^{-11}/a$.

Supplemental file 6

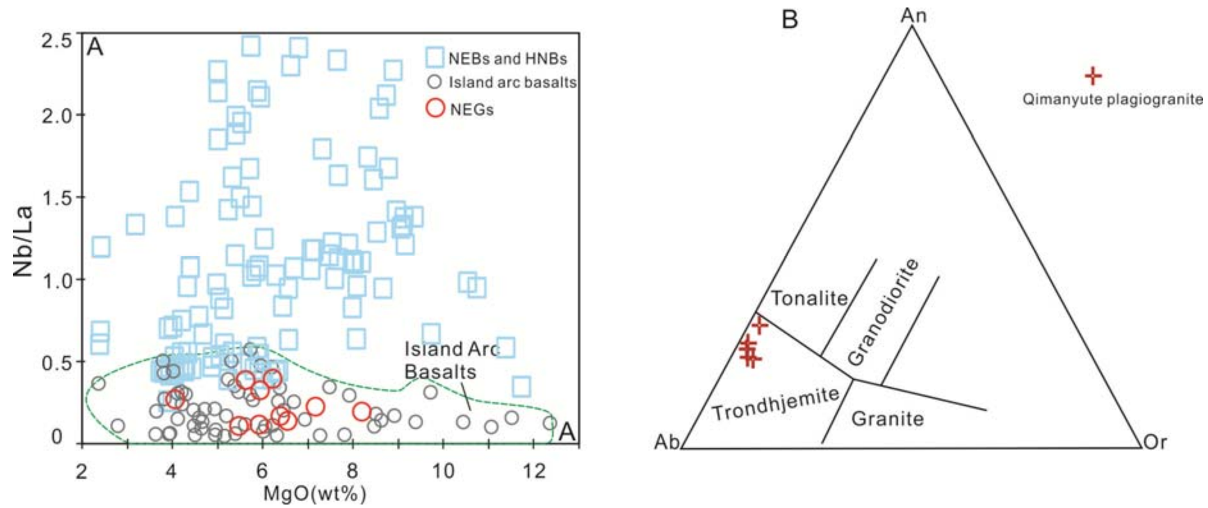

(A) MgO vs. Nb/La classification diagram (modified after Kepezhinskas et al., 1996)for the Qimanyute NEGs in the western Kunlun Orogen, NW Tibet. (B) Feldspar normative An–Or–Ab diagram (after O'Connor, 1965) for the Qimanyuteplagiogranites, showing the fields for tonalite (To), trondhjemite (Tdh), granodiorite(Gd) and granite (Gr) used in this study.The published data of HNBs and NEBs are from Reagan et al. (1989), Defant et al. (1992), Kepezhinskas et al. (1996), Sajona et al. (1996), Aguillón-Robles et al. (2001), Polat and Kerrich. (2001), Castillo et al. (2002), Gorring et al. (2003), Zhang et al. (2005), Wang et al. (2007, 2008), Petrone and Ferrari, 2008, Macphersonet al. (2010), Hastie et al. (2011), and Sorbadere et al. (2013).